Showcasing research from Prof. Nishina's laboratory, Okayama University and Prof. Minami's laboratory, The University of Tokyo, Japan.

Non-enzymatic detection of glucose levels in human blood plasma by a graphene oxide-modified organic transistor sensor

An extended-gate-type organic transistor (OFET) functionalized with an artificial receptor can selectively detect target glucose as well as minimize interferent effects such as protein adsorption on the detection electrode in human blood plasma by graphene oxide.

As featured in:

ROYAL SOCIETY OF CHEMISTRY

rsc.li/chemcomm

COMMUNICATION

Check for updates

Non-enzymatic detection of glucose levels in human blood plasma by a graphene oxide-modified organic transistor sensor†

Haonan Fan, [iD] [a] Yui Sasaki, [iD] [a] Qi Zhou, [iD] [a] Wei Tang, [iD] [a] Yuta Nishina [iD] *[bc] and Tsuyoshi Minami [iD] *[a]

We herein report an organic transistor functionalized with a phenyl-boronic acid derivative and graphene oxide for the quantification of plasma glucose levels, which has been achieved by the minimization of interferent effects derived from physical protein adsorption on the detection electrode.

The launch of the concept of point-of-care (POC) testing has vigorously promoted the development of sensor technology.[1] Among them, portable sensors for glucose are in high demand because patients with diabetes require self-checking of glucose levels in daily life.[2] In particular, diabetic complications could be caused by the fluctuation of plasma glucose levels or constant high glucose levels,[3] meaning that methods for accurate glucose monitoring are essential. Toward accurate detection of glucose in human blood samples, enzymatic sensors have been widely developed to date. The biosensors based on the detection principle of catalytic reactions of enzymes (*e.g.*, glucose oxidase) possess high selectivity and sensitivity, while interferent effects on the enzyme electrodes could be induced by oxidation of electrochemically active species (*e.g.*, ascorbic acid) in human blood samples.[4] Moreover, the instability of the biogenic recognition materials against physical and/or chemical stimuli is still a concern in the actual sensing environment.[2] Taking into consideration the robustness of the sensing system, artificial receptors[5] are promising recognition materials for real-sample analysis.[6]

The representative artificial receptor for glucose is phenyl-boronic acid (PBA),[5a,5c] which reacts with a *cis*-diol moiety

through a dynamic covalent bond. However, general artificial receptors confront issues to gain high selectivity against a specific analyte because of their inherent cross-reactivity.[6] Hence, sophisticated designs considering the conformation between the *cis*-diol moiety and the boronic acid moiety are necessary for the accurate detection of glucose.[7] Although such elaborate artificial receptors have been developed to increase the binding affinity to glucose, the influence of a large amount of interferents in human blood samples is not still ignorable. In other words, sufficient sensor designs at molecular levels to retain the favorable discrimination power in real-sample analysis are still at the frontier. To this end, we decided to change our perspective to a molecular recognition portion at a nanoscale for maximizing the selectivity of a single artificial receptor. The significant difference in nanomaterials from single artificial receptors is an extensive large surface originating from the assembled or conjugated structures.[8] Therefore, the large surface allows a sufficient number of intermolecular interactions at the interface.

A self-assembled monolayer (SAM) functionalized with a molecular recognition moiety provides a two-dimensional detection portion. Considering the nature of SAM-based chemical sensing, their selectivity is significantly influenced by the morphology of the surface.[9] Although the discrimination of the slight structural differences in saccharides is challenging in a single artificial receptor, the functionalized SAMs could tune the selectivity by the density of receptors. In this assay, a simple structural artificial receptor, 4-mercaptophenylboronic acid (4-MPBA)[10] was selected as a building block for the SAM.

Certainly, the applications of SAMs have been expanded to real-sample analysis in analytical chemistry, and an approach using SAMs has been applied to inhibit interferent effects on metal surfaces.[11] In this method, the SAMs play a role in trapping the interferent proteins,[12] whereas their inhibition ability at a large amount of interferents is limited owing to their adsorption capacity. Thus, we focused on the principle of repulsion for the minimization of interferent effects. In the case

[a] *Institute of Industrial Science, The University of Tokyo, 4-6-1 Komaba, Meguro-ku, Tokyo, 153-8505, Japan. E-mail: tminami@g.ecc.u-tokyo.ac.jp*

[b] *Research Core for Interdisciplinary Sciences, Okayama University, Okayama 700-8530, Japan*

[c] *Graduate School of Natural Science and Technology, Okayama University, Okayama 700-8530, Japan. E-mail: nisina-y@cc.okayama-u.ac.jp*

† Electronic supplementary information (ESI) available: Preparation of GO solution, fabrication and characterization details of the OFET and the extended-gate Au electrode, investigation of the detectability of the OFET-based sensor, and spike and recovery tests. See DOI: https://doi.org/10.1039/d2cc07009j

of the SAM for resistance to protein adsorption, the conformation of the terminal unit of the SAM affects the suppression ability of interferent effects,[13] whereas the control of the conformation of the SAM is difficult. Hence, a representative nanocarbon material, graphene oxide (GO), possessing multiple negative charges on the surface,[14] was employed to prevent protein adsorption on the detection portion.[15] The main target, human blood plasma, contains negatively charged proteins (e.g., immunoglobulin G and serum albumin),[16] suggesting that the interferents could be resisted on the detection portion functionalized with GO by electrostatic repulsion.[14b]

An organic field-effect transistor (OFET),[17] which is a solution-processable electronic device, shows a unique switching profile by applying a gate voltage. The molecular recognition materials can be incorporated into a gate electrode of the OFET, indicating that the functionalized OFET enables the reading out of sensing information through transistor characteristics.[10,17c] In this study, we designed an OFET connected to an extended-gate Au electrode functionalized with 4-MPBA as the glucose receptor and GO for the suppression of interferent effects (Fig. 1). By employing the OFET-based sensor functionalized with GO (GO-OFET), the glucose levels were detected in human blood plasma.

The extended-gate electrode was assembled by a thermally deposited Au, an electrochemically deposited Au nanostructure (AuNS),[18] GO, and a 4-MPBA-based SAM (Fig. S2, ESI†). The morphology of the surface of the functionalized extended-gate Au electrode was evaluated by microscopic analysis. The field-emission scanning electron microscope (FE-SEM) image of the surface of the AuNS layer on the thermally deposited Au electrode showed high surface roughness stemming from the needle-like sharp architectures[18b] (Fig. 2(a)). According to the electrochemical deposition of GO by chronoamperometry, deposits caught on the edges of the needle architectures were observed in Fig. 2(b) and (c). The edges of the needle architectures possess positive charges by the principle of electric field concentration;[19] thus, the negatively charged GO was accumulated on the AuNS layers by electrostatic interactions. Indeed, the distribution of elements in the energy dispersive X-ray (EDX)-mapping (Fig. 2(d)–(f)) corresponded to the position of GO on the AuNS layer (Fig. 2(c)). Subsequently, the modification of 4-MPBA on the extended-gate Au electrode was evaluated
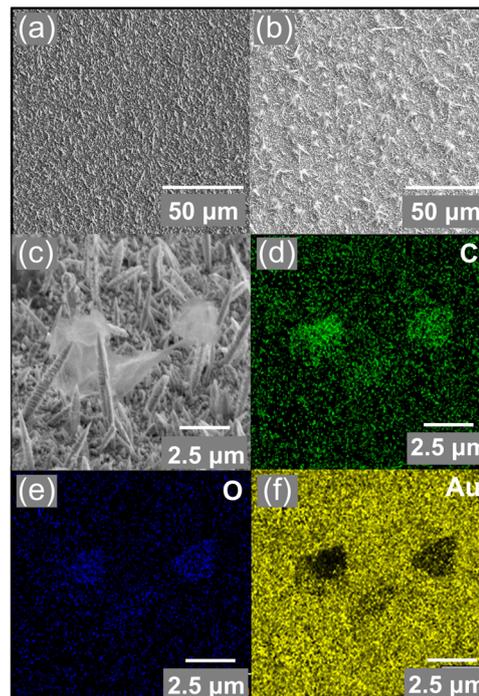

Fig. 2 FE-SEM images of the surface of the extended-gate Au electrode functionalized with (a) the AuNS layer and (b and c) the GO and AuNS layer. EDX-mapping images of (d) C, (e) O, and (f) Au for (c).

by linear sweep voltammetry (LSV), photoelectron yield spectroscopy in air, and contact angle measurements (Fig. S3–S5, ESI†). We expected that the 4-MPBA-based SAM could be formed through Au–S bonds on the bare AuNS even in the presence of GO, and the molecular density of 4-MPBA on the extended-gate Au electrode functionalized with the GO and AuNS layers was estimated to be $(8.5 \pm 0.2) \times 10^{-10}$ mol cm^{-2} (Fig. S3(a), ESI†).

After the abovementioned characterization, the detectability (i.e., selectivity, response time, and accuracy) of the OFET with the extended-gate Au electrode to interferents[20] (i.e., lactic acid,[20a] citric acid,[20b] and, ascorbic acid[20c]) and saccharides (i.e., glucose, fructose,[20d] galactose,[20e] and mannose[20f]) was examined. The manufactured OFET displayed a stable switching profile under ambient conditions, indicating its potential as a chemical sensor device (Fig. S1, ESI†). As shown in Fig. 3, the GO-OFET-based sensor exhibited the highest response to glucose over other species. In contrast to molecular recognition at a solution state, the self-assembled receptor at a solid state could provide a two-dimensional detection portion to recognize the slight difference in the saccharide structures.[10a,21] More importantly, very weak responses to interferents generally contained in human blood plasma (i.e., the organic acids[20a–c] and mannose[20f]) were observed. Namely, the GO-OFET-based sensor could discriminate the response to glucose from the interferent effects. Furthermore, the GO-OFET exhibited a moderate response to fructose (Fig. S8, ESI†), which was stemming from the inherent binding affinity of PBA derivatives.[10a] The transfer characteristics of the GO-OFET positively shifted by adding glucose in contrast to that of the OFET without GO
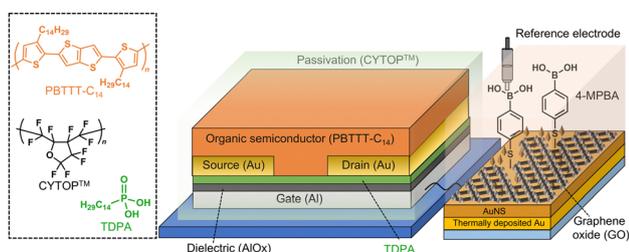

Fig. 1 Schematic illustration of the extended-gate OFET for the monitoring of plasma glucose levels. The extended-gate Au electrode was functionalized with Au nanostructures (AuNSs), graphene oxide (GO), and 4-mercapto-phenylboronic acid (4-MPBA).
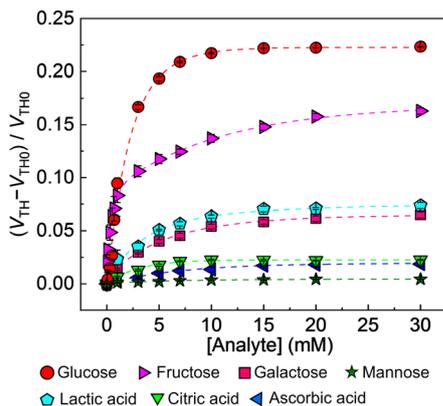
Fig. 3 Response profiles of the GO-OFET-based chemical sensor with 4-MPBA against seven analytes in 0.1 M phosphate buffer with 0.1 M NaCl at pH 7.4. Titration isotherms were obtained by collecting V_{TH} at each concentration of analytes from 0 to 30 mM. The terms V_{TH0} and V_{TH}, respectively, indicate threshold voltages before and after adding the analytes. Three repetitive evaluations were carried out for each analyte.
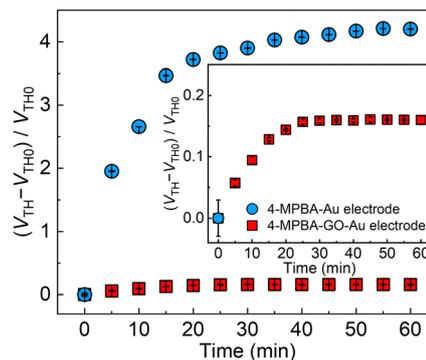

Fig. 4 Antifouling ability test for the OFET in non-diluted human blood plasma. The red squares and blue circles mean the 4-MPBA-attached extended-gate Au electrode with and without GO, respectively. Three repetitive evaluations were carried out for each electrode. Inset shows the enlarged figure for V_{TH} shifts.

(Fig. S9(a), ESI†),[10] which might be explained by the change in the surface potential of the electrode derived from proton transfer upon forming the boronate ester.[22] Moreover, a sigmoidal response to glucose was observed at a low concentration range (Fig. S7(b), ESI,† inset), implying a formation change from a 2:1 to 1:1 complex of 4-MPBA and glucose with an increase in glucose concentration.[23] Furthermore, the selectivity test showed a different response pattern to saccharides from a cross-reactive response in a previous report,[10a] which might be due to the difference in the molecular densities (Fig. S3(b), ESI†).[21a]

Next, the role of GO for the minimization of the interferent effects, such as physical protein adsorption[16] to the sensing portion, was investigated by an antifouling ability test against negatively charged proteins (i.e., immunoglobulin G and serum albumin) contained in human blood plasma. In Fig. S10 (ESI†), the OFET-based sensor without GO displayed the gradual time-dependent change in the threshold voltages in the presence of the proteins, suggesting accumulation of the negatively charged proteins on the extended-gate electrode. In contrast, a negligible response to the proteins was observed in the case of the GO-OFET. The ζ-potential of the utilized GO material represented −22.9 ± 1.4 mV at pH 7.4, whereby the suppressed response to the proteins could be explained by electrostatic repulsion between the negatively charged GO surface and the proteins. Moreover, the GO-OFET was also examined in non-diluted human blood plasma toward real-sample analysis (Fig. 4). The OFET without GO displayed much higher interferent effects stemming from the physical adsorption of the proteins to the sensing portion in human blood plasma. Meanwhile, the GO-OFET showed a moderate time-dependent response, which was derived from plasma glucose (vide infra) capturing on 4-MPBA as well as suppression of the protein adsorption by GO.

Finally, the GO-OFET was applied to the quantification of glucose levels in human blood plasma. The original concentration of plasma glucose (i.e., 4.4 ± 0.2 mM (n = 3)) was

determined by a commercial biochemical analyzer using a dry chemistry system. As shown in Fig. 5(a), the transfer curves of the GO-OFET stepwise shifted with an increase in glucose concentration. The obtained titration isotherm represented a non-linear saturation curve (Fig. 5(a), inset), which indicated
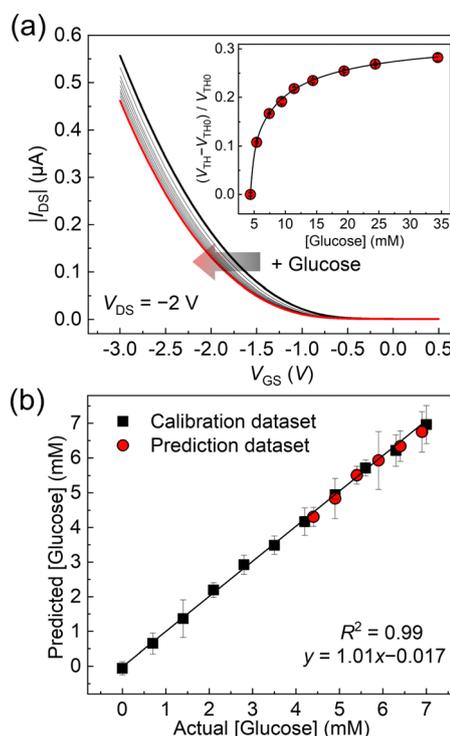

Fig. 5 (a) Transfer characteristics of the GO-OFET-based chemical sensor with 4-MPBA upon the addition of glucose in human blood plasma. The inset represents the titration isotherm obtained by collecting V_{TH} at each concentration of analytes from 4.4 to 34.4 mM with three repetitive measurements. The initial concentration means the original concentration of the plasma glucose determined by the commercial biochemical analyzer (4.4 ± 0.2 mM, (n = 3)). (b) Result of the spike and recovery test for glucose in human blood plasma. Three repetitive evaluations were carried out for each concentration.

the successful quantitative detection of glucose levels in human blood plasma. To the best of our knowledge, this is the first example to detect glucose levels in human blood plasma by using FETs functionalized with the PBA derivatives. As a further attempt, a spike and recovery test for glucose in human blood plasma was carried out (Fig. 5(b)). The glucose concentrations were predicted by utilizing the calibration line, and the recovery rates against glucose were determined to be 87–110% (Table S1, ESI†). Indeed, the predicted plasma glucose concentration by the OFET-based sensor (4.3 ± 0.27 mM, in Table S1, ESI†) was comparable to the result of the commercial biochemical analyzer. Therefore, the estimated recovery rates implied the feasibility of accurate analysis by the glucose sensor based on the GO-OFET in real-world scenarios.

In summary, we developed a GO-OFET functionalized with 4-MPBA for accurate detection of glucose levels in human blood plasma. The PBA derivatives have been widely utilized as artificial saccharide receptors, whereas the discrimination of saccharides in real samples containing large amounts of interferents has been challenging owing to the limitation of the receptor design. In our approach, we expected that the selected nanomaterial (*i.e.*, GO) could maximize the sensing ability of the OFET modified with 4-MPBA. Indeed, the GO-OFET successfully quantified glucose concentrations in human blood plasma, which was accomplished by the minimalization of the physical adsorption of the interferent proteins. Judging from the accurate detection of plasma glucose levels by the GO-OFET, we believe that it has potential for the establishment of a POC glucose device based on the fusion technology of organic electronics and nanocarbon chemistry.

Conflicts of interest

There are no conflicts of interest to declare.

References

1 V. Gubala, L. F. Harris, A. J. Ricco, M. X. Tan and D. E. Williams, *Anal. Chem.*, 2012, **84**, 487–515.
2 H. Lee, Y. J. Hong, S. Baik, T. Hyeon and D.-H. Kim, *Adv. Healthcare Mater.*, 2018, **7**, 1701150.
3 Z.-Y. Zhang, L.-F. Miao, L.-L. Qian, N. Wang, M.-M. Qi, Y.-M. Zhang, S.-P. Dang, Y. Wu and R.-X. Wang, *Front. Endocrinol.*, 2019, **10**, 640.
4 K. Dawson, M. Baudequin and A. O'Riordan, *Analyst*, 2011, **136**, 4507–4513.
5 (a) X. Wu, Z. Li, X.-X. Chen, J. S. Fossey, T. D. James and Y.-B. Jiang, *Chem. Soc. Rev.*, 2013, **42**, 8032–8048; (b) A. P. Davis, *Chem. Soc. Rev.*, 2020, **49**, 2531–2545; (c) G. T. Williams, J. L. Kedge and J. S. Fossey, *ACS Sens.*, 2021, **6**, 1508–1528.
6 (a) Y. Sasaki, É. Leclerc, V. Hamedpour, R. Kubota, S. Takizawa, Y. Sakai and T. Minami, *Anal. Chem.*, 2019, **91**, 15570–15576; (b) X. Lyu, V. Hamedpour, Y. Sasaki, Z. Zhang and T. Minami, *Anal. Chem.*, 2021, **93**, 1179–1184.
7 (a) T. D. James, K. R. A. S. Sandanayake and S. Shinkai, *Angew. Chem., Int. Ed. Engl.*, 1994, **33**, 2207–2209; (b) V. V. Karnati, X. Gao, S. Gao, W. Yang, W. Ni, S. Sankar and B. Wang, *Bioorg. Med. Chem. Lett.*, 2002, **12**, 3373–3377; (c) T. Hashimoto, M. Kumai, M. Maeda, K. Miyoshi, Y. Tsuchido, S. Fujiwara and T. Hayashita, *Front. Chem. Sci. Eng.*, 2020, **14**, 53–60.
8 K. Ariga, M. Nishikawa, T. Mori, J. Takeya, L. K. Shrestha and J. P. Hill, *Sci. Technol. Adv. Mater.*, 2019, **20**, 51–95.
9 J. Mehne, G. Markovic, F. Pröll, N. Schweizer, S. Zorn, F. Schreiber and G. Gauglitz, *Anal. Bioanal. Chem.*, 2008, **391**, 1783–1791.
10 (a) T. Minami, T. Minamiki, Y. Hashima, D. Yokoyama, T. Sekine, K. Fukuda, D. Kumaki and S. Tokito, *Chem. Commun.*, 2014, **50**, 15613–15615; (b) P. Didier, N. Lobato-Dauzier, N. Clément, A. J. Genot, Y. Sasaki, É. Leclerc, T. Minamiki, Y. Sakai, T. Fujii and T. Minami, *ChemElectroChem*, 2020, **7**, 1332–1336.
11 Y. Sato, K. Yoshioka, T. Murakami, S. Yoshimoto and O. Niwa, *Langmuir*, 2012, **28**, 1846–1851.
12 O. R. Bolduc, J. N. Pelletier and J.-F. Masson, *Anal. Chem.*, 2010, **82**, 3699–3706.
13 K. Feldman, G. Hähner, N. D. Spencer, P. Harder and M. Grunze, *J. Am. Chem. Soc.*, 1999, **121**, 10134–10141.
14 (a) Y. Nishina and S. Eigler, *Nanoscale*, 2020, **12**, 12731–12740; (b) K. Ohno, C. Zhao and Y. Nishina, *Langmuir*, 2019, **35**, 10900–10909; (c) N. D. Q. Chau, G. Reina, J. Raya, I. A. Vacchi, C. Ménard-Moyon, Y. Nishina and A. Bianco, *Carbon*, 2017, **122**, 643–652; (d) G. Reina, N. D. Q. Chau, Y. Nishina and A. Bianco, *Nanoscale*, 2018, **10**, 5965–5974; (e) M. Z. I. Nizami, Y. Nishina, T. Yamamoto, Y. Shinoda-Ito and S. Takashiba, *J. Dent. Res.*, 2020, **99**, 182–188.
15 R. Rode, M. Schmid and S. Moghaddam, *Adv. Mater. Interfaces*, 2022, **9**, 2101613.
16 S. E. Moulton, J. N. Barisci, A. Bath, R. Stella and G. G. Wallace, *J. Colloid Interface Sci.*, 2003, **261**, 312–319.
17 (a) J. Mei, Y. Diao, A. L. Appleton, L. Fang and Z. Bao, *J. Am. Chem. Soc.*, 2013, **135**, 6724–6746; (b) H. Chen, W. Zhang, M. Li, G. He and X. Guo, *Chem. Rev.*, 2020, **120**, 2879–2949; (c) R. Kubota, Y. Sasaki, T. Minamiki and T. Minami, *ACS Sens.*, 2019, **4**, 2571–2587.
18 (a) Y. Liu, Z. Liu, F. Zhao and Y. Tian, *Angew. Chem., Int. Ed.*, 2021, **60**, 14429–14437; (b) Q. Zhou, Y. Sasaki, K. Ohshiro, H. Fan, V. Montagna, C. Gonzato, K. Haupt and T. Minami, *J. Mater. Chem. B*, 2022, **10**, 6808–6815.
19 S. Otsuka, T. Shimizu, S. Shingubara, K. Makihara, S. Miyazaki, A. Yamasaki, Y. Tanimoto and K. Takase, *AIP Adv.*, 2014, **4**, 087110.
20 (a) R. B. Brandt, S. A. Siegel, M. G. Waters and M. H. Bloch, *Anal. Biochem.*, 1980, **102**, 39–46; (b) J. A. J. Trygg, J. Gullberg, A. I. Johansson, P. Jonsson, H. Antti, S. L. Marklund and T. Moritz, *Anal. Chem.*, 2005, **77**, 8086–8094; (c) S. Feng, J. Pan, Y. Wu, D. Lin, Y. Chen, G. Xi, J. Lin and R. Chen, *Sci. China: Life Sci.*, 2011, **54**, 828–834; (d) B. M. Lee and T. M. S. Woleve, *Eur. J. Clin. Nutr.*, 1998, **52**, 924–928; (e) N. Ercan, F. Q. Nuttall, M. C. Gannon, J. B. Redmon and K. J. Sheridan, *Metabolism*, 1993, **42**, 1560–1567; (f) T. Taguchi, I. Miwa, T. Mizutani, H. Nakajima, Y. Fukumura, I. Kobayashi, M. Yabuuchi and I. Miwa, *Clin. Chem.*, 2003, **49**, 181–183.
21 (a) A. Matsumoto, H. Matsumoto, Y. Maeda and Y. Miyahara, *Biochim. Biophys. Acta*, 2013, **1830**, 4359–4364; (b) T. Kajisa and T. Sakata, *ChemElectroChem*, 2014, **1**, 1647–1655; (c) S. Li, Q. Zhou, W. Chu, W. Zhao and J. Zheng, *Phys. Chem. Chem. Phys.*, 2015, **17**, 17638–17645.
22 (a) Y. Zhou, H. Dong, L. Liu, J. Liu and M. Xu, *Biosens. Bioelectron.*, 2014, **60**, 231–236; (b) B. Marco-Dufort, R. Iten and M. W. Tibbitt, *J. Am. Chem. Soc.*, 2020, **142**, 15371–15385.
23 T. Nagasaki, H. Shinmori and S. Shinkai, *Tetrahedron Lett.*, 1994, **35**, 2201–2204.